The Journal of Chemical Physics

RESEARCH ARTICLE | NOVEMBER 18 2024

A high-resolution photoelectron spectroscopic and computational study of TaX^- (X = C, N, O)

Xiaolin Chen ; Shuaiting Yan ; Rui Zhang ; Chuangang Ning

J. Chem. Phys. 161, 194305 (2024)
https://doi.org/10.1063/5.0239233

The Journal of Chemical Physics ARTICLE pubs.aip.org/aip/jcp

A high-resolution photoelectron spectroscopic and computational study of TaX^- (X = C, N, O)

Cite as: J. Chem. Phys. 161, 194305 (2024); doi: 10.1063/5.0239233
Submitted: 18 September 2024 • Accepted: 3 November 2024 •
Published Online: 18 November 2024

Xiaolin Chen,[1,a)] Shuaiting Yan,[2] Rui Zhang,[2] and Chuangang Ning[2,b)]

AFFILIATIONS

[1] College of Optical, Mechanical and Electrical Engineering, Zhejiang A&F University, Hangzhou 311300, China
[2] Department of Physics, State Key Laboratory of Low Dimensional Quantum Physics, Frontier Science Center for Quantum Information, Tsinghua University, Beijing 100084, China

[a)] **Author to whom correspondence should be addressed:** chenxl13@zafu.edu.cn
[b)] ningcg@tsinghua.edu.cn

ABSTRACT

We report on the high-resolution photoelectron spectroscopy of diatomic molecules TaX^- (X = C, N, O) anions using a cryogenic ion trap combined with the slow electron velocity imaging (cryo-SEVI) method. We determined the electron affinities of TaC, TaN, and TaO to be 2.098(2), 1.576(2), and 1.069(2) eV, respectively. In addition, the electron affinities of TaX molecules were calculated using the CCSD(T) method with the complete basis sets. To interpret the complicated photoelectron spectra, we predicted the excited states of TaX molecules using the MRCI + Q method, accounting for the spin–orbit coupling effects. Several new excited states of these molecules were observed.

I. INTRODUCTION

Transition metal (TM) compounds are important functional materials with significant applications in fields such as magnetism, catalysis, and superconductivity.[1–3] Due to the partially filled *d* orbitals of TM elements, the electronic structures of TM compounds are notably complex. This complexity is particularly pronounced for the 5d group elements, where the large atomic number and heavy mass lead to more pronounced spin–orbit coupling effect compared to the 3d and 4d groups. The competitions between spin–orbit coupling effects, electron correlations, and lattice interactions endow 5d TM compounds with a rich array of quantum properties.[4] Understanding the electronic structure of these compounds is therefore essential for elucidating their diverse properties.

This work investigates the photoelectron spectrum (PES) of TaX^- (X = C, N, O), which represents the simplest molecular system among TM compounds. Studying these diatomic molecules is helpful in understanding more complex systems.[5–7] In addition, the heavy polar molecule TaN has been identified as a promising candidate for the electron electric dipole moment (eEDM) experiment.[8,9] Due to the atypical conditions required for the formation of group 3–5 monocarbides, they are more challenging to generate compared to group 8–10 monocarbides.[10] This is also why there have been reported only a few spectroscopic experiments. Recently, Nakhate *et al.* investigated the electronic structure of TaC through laser-induced fluorescence (LIF) spectroscopy.[11] They determined the vibrational frequency of the ground state $^2\Sigma^+$ to be 769.1(1) cm^{-1}. Wang *et al.* theoretically investigated the ground-state structures of neutral, cationic, and anionic TaC using the density functional theory (DFT) method[12] and predicted the electron affinity (EA) value for TaC to be 2.24 eV. Majumdar and Balasubramanian employed the multireference configuration interaction (MRCI) method to study the potential energy curves and spectroscopic constants of TaC and TaC^+, suggesting a ground-state vibrational frequency of 748 cm^{-1}.[13] The only experimental study on TaC^- anion was conducted by Aravind *et al.* using photoelectron spectroscopy.[14] They measured the EA value of TaC as 1.928(0.056) eV. They also measured the ground-state vibrational frequency of TaC as 1064 cm^{-1}, which contrasts with the experimental result of 769.1(1) cm^{-1} by Nakhate *et al.*[11,14]

Ram *et al.* first used a Fourier-transform spectrometer (FTS) to study the emission spectrum of TaN in the 3000–35 000 cm^{-1} range and employed the MRCI method to calculate the molecular electronic states.[15] The first excited state $^3\Delta_1$ of TaN was experimentally determined to be 2827 cm^{-1} higher than the ground state. Starting from 2016, several groups reported the LIF experiments of TaN molecules, determining their spectroscopic constants, the branching ratios, and transition dipole moments for the $^3\Delta$ and $^1\Delta$ states.[16–20]

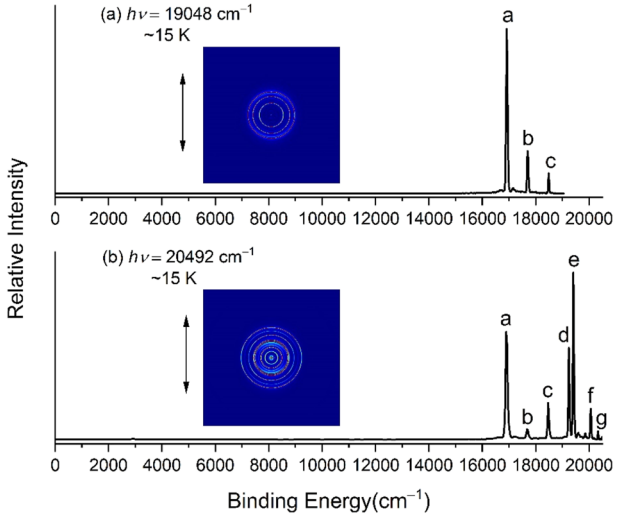

FIG. 1. Photoelectron images and spectra of cryogenically cooled TaC^- about 15 K at photodetachment energies (a) 19 408 cm^{-1} and (b) 20 492 cm^{-1}. The double arrow indicates the laser polarization.

On the theoretical side, Fleig *et al.* performed all-electron calculations including spin–orbit interactions for the ground and excited states of TaN.[9] The only experimental study on TaN^- anions is the photoelectron spectroscopy reported by Valdivielso using the velocity-map imaging method. They determined the EA value of TaN to be 1.574(1) eV.[21]

In 1967, Cheetham and Barrow studied the fluorescence spectrum of TaO in the gas phase and identified its ground state as X $^2\Delta_{3/2}$, the vibration frequency ω_e to be 1028.69 cm^{-1}, and the splitting of $^2\Delta$ to be 3505 cm^{-1} (0.4346 eV).[22] Ram *et al.* and Al-Khalili *et al.* studied the high-resolution emission spectrum of TaO using a Fourier transform spectrometer (FTS).[23–25] Recently, Thomas *et al.* used laser excitation spectroscopy to perform the rotation and hyperfine analysis of the D $^2\Pi_{1/2}$–X $^2\Delta_{3/2}$ (0,0) and E $^2\Pi_{1/2}$–X $^2\Delta_{3/2}$ (1,0) bands of TaO, further improving the accuracy of the energy levels.[26–28] On the theoretical side, the focus of the research is on the ground state X $^2\Delta$ and the lower excited state $^4\Sigma^-$ of TaO.[29–32] Dolg *et al.* used CASSCF/MRCI to study two excited states. The calculation showed that the energy of $^4\Sigma^-$ is 0.76 eV higher than the ground state, and the spin–orbit coupling splitting of the ground state $^2\Delta$ was calculated to be 3567 cm^{-1}.[31] Recently, Wu *et al.* calculated the vibration frequency of TaO, TaO^+, and TaO^- based on the density functional method BP86/LAN2DZ.[32] They predicted the electron affinity of TaO to be 0.998 eV and an excited state $^4\Sigma^+$ with an energy of 0.46 eV higher than the ground state. The latest experimental result of the EA value of TaO is by Zheng *et al.* using the magnetic bottle photoelectron spectroscopy in 2008. They obtained EA(TaO) = 1.07 ± 0.06 eV.[33]

Although these molecules have been extensively studied, their ion energetic data require more precise measurements, and their electronic states are not well clarified. The slow-electron velocity-map imaging method combined with the cryogenic ion trap (cryo-SEVI) has shown great advantages for studying complex molecular systems due to its high energy resolution.[34–40] Here, we employed the cryo-SEVI photoelectron spectroscopy of TaX^- (X = C, N, O) alongside the high level quantum chemical calculations to investigate the electronic states and vibrational states of TaX. The high level CCSD(T)/CBS calculations were employed to optimize the geometries and calculate the EA values and the vibration frequency. The MRCI method, incorporating the spin–orbit coupling effects, was applied to calculate the excited states.

II. METHODS

A. Experimental method

The experimental setup used in this study has been described in detail elsewhere.[39,41–43] Briefly, TaX (X = C, N, O) anions were produced by focusing a pulsed 532-nm laser onto a tantalum metal disk (purity 99.99%) with N_2O or CH_4 as the reaction gas. The generated anions were guided into a homemade radio frequency (rf) octupole ion trap, which was mounted on a cryogenic cold head with a temperature held at 15 or 7 K. The trapped ions were cooled down to their vibrational ground states and a few low rotational states through the collisions with the buffer gas (80%He + 20%H_2). After a trapping period of 45 ms, the interested anions were ejected out and selected using a Wiley–McLaren type time-of-flight (TOF) mass spectrometer.[44] They were then photodetached in the interaction zone of the velocity-map imaging lens. The

TABLE I. Measured binding energy (BE), the energy shift from the ground-state neutral TaC, the assignment, and the anisotropy parameter β of each observed peak for TaC^- in Fig. 1. All β values are the results at $h\nu$ = 24 092 cm^{-1}. Accurate optical shift is the results obtained by Nakhate *et al.* through the study of TaC using LIF.[11]

Peak	BE (cm^{-1})	Shift (cm^{-1})	Accurate optical shift (cm^{-1})	Assignment	β
a	16 918(16)	0		X $^1\Sigma^+ \rightarrow$ X $^2\Sigma^+$ 0 → 0	1.2
b	17 700(16)	782(23)	769.1(1)[11]	X $^1\Sigma^+ \rightarrow$ X $^2\Sigma^+$ 0 → 1	0.6
c	18 478(16)	1560(23)	1548(20)[11]	X $^1\Sigma^+ \rightarrow$ X $^2\Sigma^+$ 0 → 2	0.9
d	19 245(16)	2327(23)	2313(20)[11]	X $^1\Sigma^+ \rightarrow$ X $^2\Sigma^+$ 0 → 3	1.0
e	19 410(16)	2492(23)	2451(20)[11]	X $^1\Sigma^+ \rightarrow$ $^4\Delta_{1/2}$ 0 → 0	1.2
f	20 061(16)	3143(23)		X $^1\Sigma^+ \rightarrow$ X $^2\Sigma^+$ 0 → 4	0.2
g	20 333(16)	3415(23)		X $^1\Sigma^+ \rightarrow$ $^4\Delta_{1/2}$ 0 → 1	−0.2

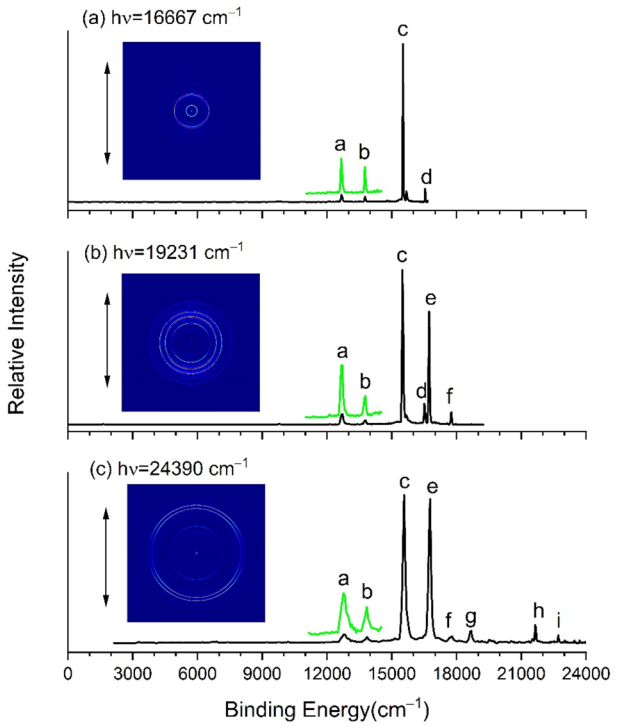

FIG. 2. Photoelectron images and spectra of TaN^- at photodetachment energies (a) 16 667 cm^{-1}, (b) 19 231 cm^{-1}, and (c) 24 390 cm^{-1} cryogenically cooled about 15 K. The double arrow indicates the laser polarization.

photodetachment laser was the optical parametric oscillator (OPO) laser pumped by the third harmonic of a neodymium:yttrium-aluminum-garnet (Nd:YAG) laser, with a linewidth of 4–8 cm^{-1} depending on the wavelength. The outgoing photoelectrons were detected using a microchannel-plate enhanced phosphor screen and recorded with a charge-coupled device (CCD) camera in an event-count mode. The photoelectron distribution was reconstructed from the accumulated imaging via the maximum entropy velocity Legendre reconstruction (MEVELER) method.[45]

For the single photon detachment with a linearly polarized laser, the photoelectron angular distribution (PAD) can by described by the following formula:[46–48]

$$\frac{d\sigma}{d\Omega} = \frac{\sigma_{tot}}{4\pi}\left(1 + \beta\left(\frac{3}{2}\cos^2\theta - \frac{1}{2}\right)\right), \quad (1)$$

where σ_{tot} is the total photodetachment cross section, β is the anisotropy parameter, and θ is the angle between the photoelectron outgoing direction and the laser polarization. The value of β is in the range of −1 to 2, depending on the kinetic energy of photoelectrons and the symmetry of the electronic state. PAD is helpful for the state assignment.

B. Computational methods

In this work, the computational study employed the all-electron augmented valence polarized sets with additional diffuse function basis sets aug-cc-pVXZ (X = T, Q, 5) for the C, N, and O atoms.[49] For tantalum, the atomic orbitals were described by the SDD (Stuttgart–Dresden effective core potential), which includes a Stuttgart-type core (60 core electrons) and relativistic effective core potential (ECP).[50] The CCSD(T) method was utilized to optimize the ground-state geometries and calculate the ground-state vibrational frequencies.[51] The structural optimization and the frequency analysis of the neutral and anionic TaX (X = C, N, O) were performed using the Gaussian 09 program.[52] The zero-point energy (ΔZPE) corrections for TaX and TaX^- were computed at the CCSD(T) level, using the aug-cc-pVTZ basis set for C, N, O and aug-cc-pVTZ-PP basis set for Ta.

The basis set extrapolation (BSE) technique was employed in high-accuracy energy calculations to minimize the residual errors arising from insufficient basis sets. By knowing the mathematical form of convergence trends, results obtained from smaller basis sets can be extrapolated to larger basis sets and even to the complete basis set (CBS) limit. To achieve more precise data, the total energy is extrapolated to the CBS limit using two different extrapolation

TABLE II. Measured binding energy (BE), the energy shift from the ground-state of neutral TaN, the assignment, and the anisotropy parameter β of each observed peak for TaN^- in Fig. 2. The β values are the results at $h\nu$ = 24 390 cm^{-1} except for peak *d*, which is at $h\nu$ = 16 667 cm^{-1}. Accurate optical shift is the results obtained by Mukund *et al.* and Bouchard *et al.* through the study of TaN using LIF.[16,17]

Peak	BE (cm^{-1})	Shift (cm^{-1})	Accurate optical shift (cm^{-1})	Assignment	β
a	12 677(40)	0		$X\ ^2\Delta_{3/2} \rightarrow X\ ^1\Sigma^+\ 0 \rightarrow 0$	−0.4
b	13 764(31)	1087(51)	1072.4(2)[16]	$X\ ^2\Delta_{3/2} \rightarrow X\ ^1\Sigma^+\ 0 \rightarrow 1$	0.7
c	15 518(19)	2841(44)	2833(4)[17]	$X\ ^2\Delta_{3/2} \rightarrow\ ^3\Delta_1\ 0 \rightarrow 0$	1.4
d	16 547(16)	3870(43)	3837(4)[17]	$X\ ^2\Delta_{3/2} \rightarrow\ ^3\Delta_1\ 0 \rightarrow 1$	0.1
e	16 726(28)	4049(49)	4023(4)[17]	$X\ ^2\Delta_{3/2} \rightarrow\ ^3\Delta_2\ 0 \rightarrow 0$	1.2
f	17 754(21)	5077(45)	5070(4)[17]	$X\ ^2\Delta_{3/2} \rightarrow\ ^3\Delta_2\ 0 \rightarrow 1$	0.2
g	18 654(55)	5977(68)		$X\ ^2\Delta_{3/2} \rightarrow\ ^3\Delta_3\ 0 \rightarrow 0$	−0.4
h	21 654(30)	8977(50)			1.2
i	22 713(22)	10 036(46)			1.0

formulas:[53,54] the two-parameter CBS extrapolation formula (CBS2), given by

$$E_n = E_{CBS2} + B \times n^{-3} \quad (n = 4, 5), \tag{2}$$

and the three-parameter CBS extrapolation formula (CBS3), given by

$$E_n = E_{CBS3} + Be^{-(n-1)} + Ce^{-(n-1)^2} \quad (n = 3, 4, 5). \tag{3}$$

Since the optimal extrapolation scheme can vary depending on the molecule and the basis set,[55,56] the results of two equations are averaged to obtain the more accurate CBS limit.

In this work, the excited states of TaX (X = C, N, O) and TaX^- were calculated using the MOLPRO program package.[57] The heteronuclear diatomic molecules, TaX/TaX^-, belong to the $C_{\infty v}$ point group. However, due to MOLPRO's limitation to Abelian point groups, we utilized the C_{2v} point group as an alternative. The computational procedure began with obtaining initial wavefunctions for the ground state using the Hartree–Fock method, followed by wavefunction optimization with the Complete Active Space Self-Consistent Field (CASSCF) approach. With the optimized wavefunction as a reference, the MRCI method, including the Davidson correction (+Q),[58] was employed to calculate the spin–orbit coupling (SOC) splitting via the Breit–Pauli SOC operator.[59] The choice of the active space is crucial for MRCI calculations. The 5*s*5*p* orbitals of Ta atom were treated as doubly occupied closed-shell orbitals, while the 1*s* orbitals of C, N, and O atoms were frozen. The ten active orbitals consisted of the 5*d*6*s* orbitals of Ta atom and the 2*s*2*p* orbitals of C and N atoms. For TaO/TaO^- molecules, the doubly occupied closed-shell orbitals included the 5*s*5*p* orbitals of Ta atom and the 2*s* orbital of O atom, while the 1s orbital of O atom was frozen. The nine active orbitals consisted of the 5*d*6*s* orbitals of Ta atom and the 2*p* orbitals of O atom.

III. RESULTS AND DISCUSSION

A. Photoelectron imaging of TaC^-

Figures 1(a) and 1(b) show the photoelectron spectra of TaC^- at a laser photon energy of $h\nu$ = 19 048 and 20 492 cm^{-1}, respectively, with the ion trap temperature at 15 K. The ground state of TaC^- is $(1\sigma)^2(2\sigma)^2(3\sigma)^2(1\pi)^4\ ^1\Sigma^+$, while the neutral ground state is $(1\sigma)^2(2\sigma)^2(3\sigma)^1(1\pi)^4\ ^2\Sigma^+$. Based on the extrapolation formulas (2) and (3), the EA of TaC was calculated to be 2.135 eV, and the vibrational frequency of the neutral ground state was calculated to be 857 cm^{-1} using the CCSD(T) method. Peak *a* in Fig. 1 corresponds to the 0–0 transition from TaC^- to the ground electronic state. The binding energy of peak *a* is the EA value and is determined to be 16 918(16) cm^{-1} or 2.098(2) eV. The recent experimental EA result 1.928(56) eV by Aravind *et al.* is not consistent with our result.[14]

The spacing between peaks *a* and *b* is equal to the vibrational frequency of the neutral ground state and was measured as 782(23) cm^{-1}. This is inconsistent with our computational results 857 cm^{-1} using CCSD(T) and the experimental result 1064 cm^{-1} by Aravind *et al.*[14] However, it agrees with the recent experimental results by Nakhate *et al.*,[11] which reported a value of 769.1(1) cm^{-1}. Instead, we calculated the potential energy curve of TaN using the MRCI calculation with the spin–orbit coupling effect and then fitted it with a Morse potential.[60] We obtained ω_e of TaC to be 784.5 cm^{-1}. This value is in good agreement with our work and Nakhate *et al.* experiment.[11] To assign these peaks, we simply followed the assignments of previous high-resolution optical spectroscopic work. It is difficult to make an undisputed assignment using one electron transition term due to the significant state mixing. The strong peaks *d* and *e* are unexpected according to the normal Franck–Condon principle and the single electron transition rule, which may be due to the coupling of two vibronic states since their energies are very close. In Nakhate's article,[11] the intensity did not align with the normal FC simulation either. The binding energies and assignment for peaks *a*–*g* are listed in Table I along with a comparison with term energies determined by LIF results by Nakhate *et al.*[11]

B. Photoelectron imaging of cold TaN^-

Figures 2(a)–2(c) show the photoelectron spectra of TaN^- at photon energies $h\nu$ = 16 667, 19 231 cm^{-1}, and 24 390 cm^{-1},

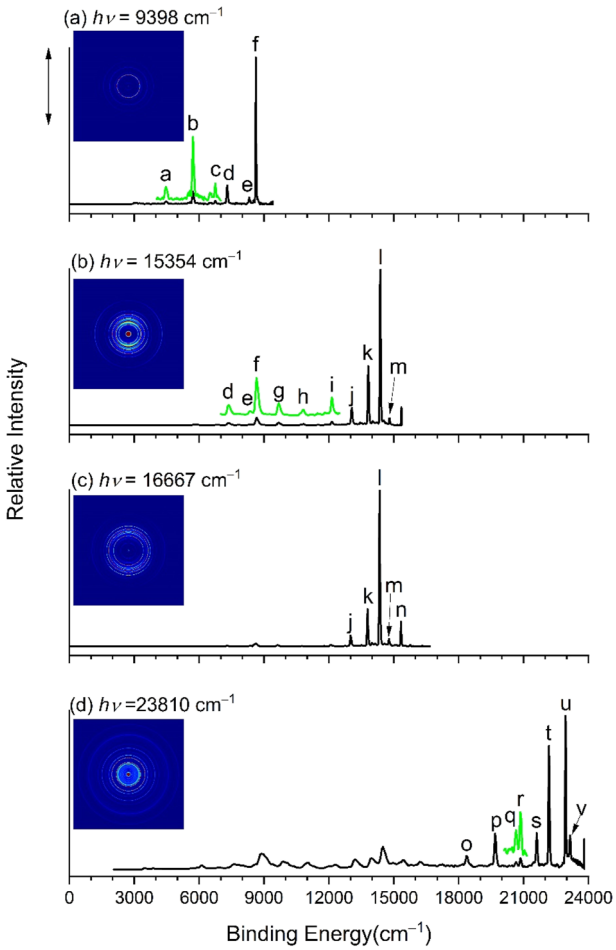

FIG. 3. Photoelectron images and spectra of TaO^- at photodetachment energies (a) 9 398 cm^{-1}, (b) 15 354 cm^{-1}, (c) 16 667 cm^{-1}, and (d) 23 810 cm^{-1} cryogenically cooled about 7 K. The double arrow indicates the laser polarization.

TABLE III. Measured binding energy (BE), the energy shift from the ground-state of neutral TaO, the assignment, and the anisotropy parameter β of each observed peak for TaO^- in Fig. 3. β values of peaks *a–f* are results at $h\nu$ = 9398 cm^{-1}, peaks *g–m* at $h\nu$ = 15 354 cm^{-1}, peaks *n* at $h\nu$ = 16 667 cm^{-1}, and peaks *o–v* at $h\nu$ = 23 810 cm^{-1}. Accurate optical shift is the results obtained by Al-Khalili through the study of TaO using FTS and by Manke *et al.* and Tovar *et al.* using laser excitation spectroscopy.[25,26,28]

Peak	BE (cm^{-1})	Shift (cm^{-1})	Accurate optical shift (cm^{-1})	Assignment	β
a	4472(28)	−4147(32)		$A\,^3\Phi_3 \rightarrow X\,^2\Delta_{3/2}\ 0 \rightarrow 0$	0
b	5718(23)	−2901(28)		$A\,^3\Phi_2 \rightarrow X\,^2\Delta_{3/2}\ 0 \rightarrow 0$	−0.3
c	6746(20)	−1873(26)		$A\,^3\Phi_2 \rightarrow X\,^2\Delta_{3/2}\ 0 \rightarrow 1$	−0.6
d	7296(19)	−1323(25)		$X\,^3\Sigma_1^- \rightarrow X\,^2\Delta_{3/2}\ 0 \rightarrow 0$	−0.2
e	8321(19)	−298(25)		$X\,^3\Sigma_1^- \rightarrow X\,^2\Delta_{3/2}\ 0 \rightarrow 1$	−0.3
f	8619(16)	0	0	$X\,^3\Sigma_0^- \rightarrow X\,^2\Delta_{3/2}\ 0 \rightarrow 0$	−0.1
g	9687(52)	1068(54)	1 029.815 3(11)[25]	$X\,^3\Sigma_0^- \rightarrow X\,^2\Delta_{3/2}\ 0 \rightarrow 1$	−0.5
h	10 802(44)	2183(47)		$X\,^3\Sigma_0^- \rightarrow X\,^2\Delta_{3/2}\ 0 \rightarrow 2$	−0.2
i	12 141(30)	3522(34)	3 505.564 8[25]	$X\,^3\Sigma_0^- \rightarrow X\,^2\Delta_{5/2}\ 0 \rightarrow 0$	0.4
j	13 053(20)	4434(26)		$X\,^3\Sigma_1^- \rightarrow a\,^4\Sigma^-\ 0 \rightarrow 0$	1.4
k	13 822(14)	5203(21)			1.2
l	14 375(8)	5756(18)		$X\,^3\Sigma_0^- \rightarrow a\,^4\Sigma^-\ 0 \rightarrow 0$	0.9
m	14 801(8)	6182(18)			0.7
n	15 331(38)	6712(41)		$X\,^3\Sigma_0^- \rightarrow a\,^4\Sigma^-\ 0 \rightarrow 1$	0
o	18 376(31)	9757(35)		$X\,^3\Sigma_1^- \rightarrow A'\,^2\Pi_{1/2}\ 0 \rightarrow 0$	−0.1
p	19 691(25)	11 072(30)	11 063[25]	$X\,^3\Sigma_0^- \rightarrow A'\,^2\Pi_{1/2}\ 0 \rightarrow 0$	0
q	20 653(22)	12 034(27)	12 017[25]	$X\,^3\Sigma_0^- \rightarrow A'\,^2\Pi_{1/2}\ 0 \rightarrow 1$	−0.2
r	20 860(21)	12 241(26)		$X\,^3\Sigma_1^- \rightarrow C\,^2\Delta_{3/2}\ 0 \rightarrow 0$	0
s	21 609(19)	12 990(25)		$X\,^3\Sigma_1^- \rightarrow D\,^2\Pi_{1/2}\ 0 \rightarrow 0$	0
t	22 175(18)	13 556(24)	13 569.257 75(13)[26]	$X\,^3\Sigma_0^- \rightarrow C\,^2\Delta_{3/2}\ 0 \rightarrow 0$	0
u	22 937(17)	14 318(23)	14 332.420 64(28)[28]	$X\,^3\Sigma_0^- \rightarrow D\,^2\Pi_{1/2}\ 0 \rightarrow 0$	0.1
v	23 146(16)	14 527(23)		$X\,^3\Sigma_0^- \rightarrow C\,^2\Delta_{3/2}\ 0 \rightarrow 1$	0

respectively, with the ion trap temperature at 15 K. The green curves in Fig. 2 represent the magnified results of the weak peaks *a* and *b* by a factor of 5. Peak *a* corresponds to the 0–0 transition from the ground state TaN^- to the neutral ground, and its binding energy, EA(TaN), is determined to be 12 677(40) cm^{-1}. According to our experimental results listed in Table II and spectroscopic data of TaN by Bouchard *et al.*,[17] we can determine that the final state of peak *d*, which has the minimum width, is the neutral excited state a $^3\Delta_1(v = 1)$, which is 3837(4) cm^{-1} higher than the neutral ground state X $^1\Sigma^+(v = 0)$. As a result, we can also obtain a more accurate EA value 12 710(16) cm^{-1} or 1.576(2) eV from the sharp peak *d*. This is in excellent agreement with the recent experimental result of 1.574(1) eV by Valdivielso.[21]

The anionic ground state is $(2\sigma)^2(3\sigma)^2(1\delta)^1\ ^2\Delta_{3/2}$, while the neutral ground state is $(2\sigma)^2(3\sigma)^2\ ^1\Sigma^+$. Based on formulas (2) and (3), the EA of TaN was theoretically determined to be 1.376 eV using CCSD(T)/CBS. It has a quite large deviation of 0.2 eV, or 4.61 kcal/mol from the experimental result. Peaks *a* and *b* are the photodetachment result of a δ molecular orbital from the ground state of the anion $^2\Delta_{3/2}$. δ molecular orbital is similar to the atomic *d* orbital with a very small photodetachment cross section, explaining why peaks *a* and *b* are very weak. The energy gap between peaks *a* and *b* corresponds to the vibrational frequency of TaN in its ground state. The measured value is 1087(51) cm^{-1}, in good agreement with the calculated value of 1079 cm^{-1} using the CCSD(T) method, as well as the experimental value of 1072.4(2) cm^{-1} from the laser-induced dispersed fluorescence spectra by Mukund *et al.*[16] Ram *et al.* also performed MRCI with spin–orbit coupling calculations of TaN.[15] Their computational results indicated that the TaN has five electronic states X $^1\Sigma^+$, $^3\Delta_1$, $^3\Delta_2$, $^3\Delta_3$, and $^1\Delta_2$ below 15 000 cm^{-1} in the energy order from low to high. Based on the theoretical calculations and previous experimental results, the assignments of peaks *a–g* are listed in Table II.[16,17] For the strong peaks *c* and *e*, the β values are 1.4 and 1.2 at $h\nu$ = 24 390 cm^{-1}, respectively. This is consistent with the photodetachment of a σ orbital, an atomic *s*-type like orbital. The kinetic energy for peak *d* is close to zero at $h\nu$ = 16 667 cm^{-1}, much lower than that of peak *c*, which is the reason why peak *d* has a very different β value from that of peak *c*. It should be noted that it is still a challenge to quantitatively calculate β values for these strongly correlated systems. There is no simple straight method to explain β values due to vibronic coupling and multi-reference characteristics of those states at the current stage. Peaks *h* and *i* might be from the same electronic state with a term energy of 8977(50) cm^{-1}. The energy gap between peaks *h* and *i* is 1059(37) cm^{-1}, close to the vibrational energy of TaN at its ground state. However, its term energy 8977(50)

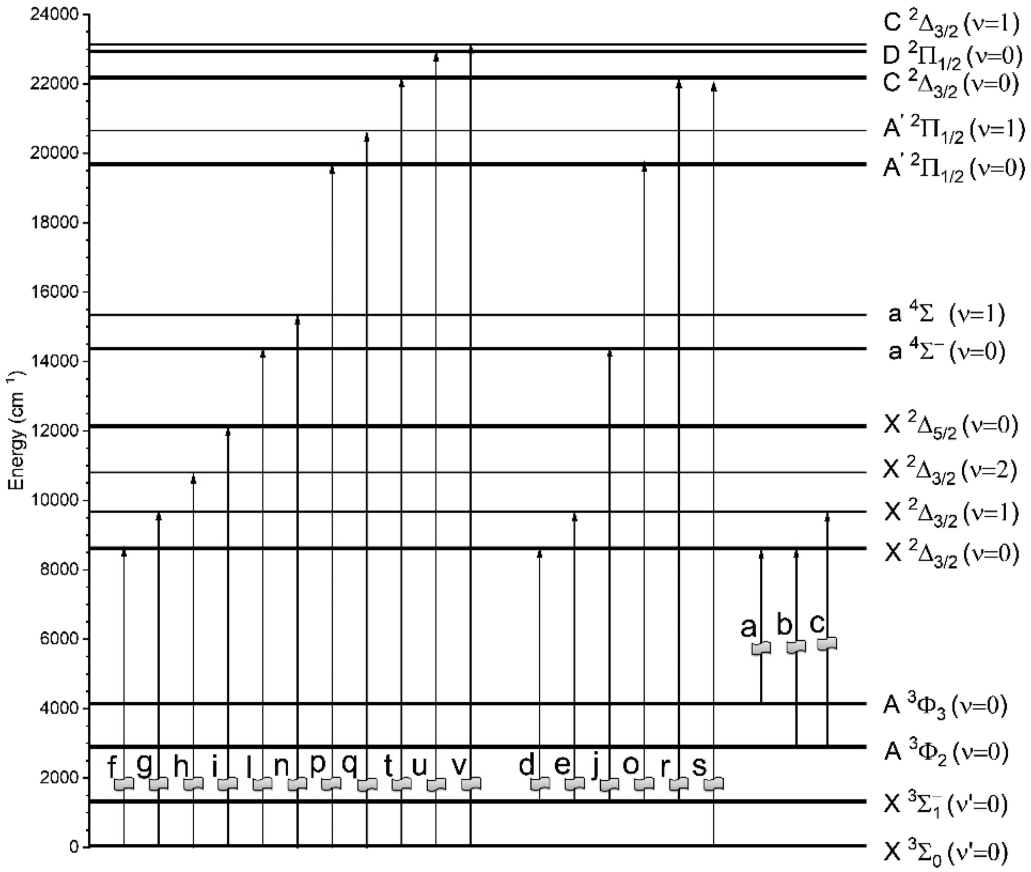

FIG. 4. Energy levels related to the observed transitions of TaO and TaO^-. The transition labels are the same as the indices of peaks in Fig. 3.

cm^{-1} is significantly different from the term energy 11 925(5) cm^{-1} of $^1\Delta_2$ determined by Valdivielso.[21] At the current stage, we cannot assign peaks *h* and *i* to any known states since there are no other states in this energy range according to the calculation by Fleig *et al.*[9]

C. Photoelectron imaging of cold TaO^-

Figures 3(a)–3(d) show the photoelectron spectra of TaO^- at photon energies $h\nu$ = 9398, 15 354, 16 667, and 23 810 cm^{-1}, respectively, with the ion trap temperature at 7 K. The green curves in Fig. 3 represent the magnified results of the weak peaks by a factor of 5. The measured results and assignment for peaks *a*–*v* are listed in Table III, and they are compared with the results of previous studies on TaO using FTS and laser excitation spectroscopy.[25,26,28] Figure 4 presents an energy level diagram of transitions from TaO^- to TaO based on the identified peaks in Table III. The ground state of TaO^- is $(15\sigma)^2(16\sigma)^2(8\pi)^4(4\delta)^2(17\sigma)^2\ X\ ^3\Sigma^-$, while $(15\sigma)^2(16\sigma)^2(8\pi)^4(4\delta)^1(17\sigma)^2\ ^2\Delta_{3/2}$ for the neutral ground state. Based on the earlier results by the Zheng group and the theoretical calculations using CCSD(T)/CBS in the present work,[33] peak *f* is assigned to the transition from the ground state of the negative ion $X\ ^3\Sigma_0^-\ v' = 0$ to the ground state of the neutral species $X\ ^2\Delta_{3/2}\ v = 0$ with a δ molecular orbital detached. This is consistent with the weak intensity of peak *f* and its anisotropy parameter $\beta = -0.1$. Peaks *g* and *h* can be assigned as transitions $X\ ^2\Delta_{3/2}\ v = 1 \leftarrow X\ ^3\Sigma_0^-\ v' = 0$ and $X\ ^2\Delta_{3/2}\ v = 2 \leftarrow X\ ^3\Sigma_0^-\ v' = 0$, respectively. The binding energy of peak *f*, measured from Fig. 3(a), is 8619(16) cm^{-1}, which corresponds to the electron affinity of TaO. By increasing the photodetachment laser energy, we have observed numerous new peaks. This represents the most complex spectrum of diatomic anions observed so far in our experiment. Our current MRCI calculation is inadequate for identifying the transitions associated with these peaks. Fortunately, through FTS experiments conducted by Al-Khalili *et al.* and Manke *et al.* have accurately determined some excited states of TaO, including $X\ ^2\Delta_{5/2}(v = 0)$, $A'\ ^2\Pi_{1/2}(v = 0)$, $C\ ^2\Delta_{3/2}$, and $D\ ^2\Pi_{1/2}(v = 0)$, which are higher in energy than the ground state by 3505.5648, 11 063, 13 569.257 75(13), 14 332.420 64(28) cm^{-1}, respectively.[22,25–28,61] The sharp strong peaks *t* and *u* in Fig. 3(d) correspond to the transitions $X^3\Sigma_0^-\ 0 \rightarrow C\ ^2\Delta_{3/2}\ 0$ and $X^3\Sigma_0^-\ 0 \rightarrow D\ ^2\Pi_{1/2}\ 0$. Thus, we can also use peaks *t* and *u* to determine the EA value. The binding energy of peak *t* is measured to be 22 175(18) cm^{-1}, and $C\ ^2\Delta_{3/2}$ is

TABLE IV. Experimental and theoretical EA values (eV), vibrational frequencies ω_e (cm^{-1}), and equilibrium bond lengths r_e (Å) for TaX (X = C, N, O) molecules in comparison with previous studies.

	TaC^-	TaC	TaN^-	TaN	TaO^-	TaO
			Previous results			
EA calc'd		1.917,[14] 2.24[12]		1.7[63]		0.998[32]
ω_e calc'd		925,[14] 748[13]		1098,[63] 1049[15]		1036.6,[61] 1070,[29] 1034,[31] 1036.5[32]
EA exp.		1.928(56)[14]		1.574(1)[21]		1.070(60)[33]
ω_e exp.		1064,[14] 769.1(1)[11]		1102.7,[64] 1070,[15] 1064.3,[16] 1073[17]		1028.69,[22] 1028.9060(15),[23] 1028.8937(11)[25]
			This work			
EA calc'd		2.085[a]		1.376[a]		1.049[a]
r_e calc'd[b]		1.754[b]		1.710[b]		1.696[b]
ω_e calc'd	987[c]	857[c], 784.5[d]	1105[c]	1079[c]	937[c]	1040[c]
ω_e exp.		782(23)		1087(51)		1068(54)
EA exp.		16 918(16)[e] 2.098(2)[a]		12 710(16)[e] 1.576(2)[a]		8619(16)[e] 1.069(2)[a]

[a]Unit eV.
[b]Method CCSD(T)/CBS.
[c]Method CCSD(T)/aug-cc-pVTZ(PP).
[d]MRCI-SO.
[e]Unit cm^{-1}.

13 569.257 75 (13) cm^{-1} higher than the ground state. As a result, EA(TaO) = 22 175(18) − 13 569.257 75(13) = 8605(18) cm^{-1}. The binding energy of peak *u* is measured to be 22 937(17) cm^{-1}, and D $^2\Pi_{1/2}$ is 14 332.420 64(28) higher than the ground state. As a result, EA(TaO) = 22 937(17) − 14 332.420 64(28) = 8605(17) cm^{-1}. The EA value of TaO from these three peaks is self-consistent. Since peak *f* has the minimum width, we recommend 8619(16) cm^{-1} or 1.069(2) eV for EA(TaO).

The energy gap between peaks *f* and *g* determined the vibrational frequency ω_e of the ground state X $^2\Delta_{3/2}$ of TaO as 1068(54) cm^{-1}, consistent with the measurement by Cheetham and Barrow in the gas phase ω_e = 1028.69 cm^{-1}.[22] In addition, the computed value 1039.5 cm^{-1} using the CCSD(T) method is also in agreement. According to MRCI calculations, the splitting of the neutral ground state X $^2\Delta$ into $^2\Delta_{3/2}$ and $^2\Delta_{5/2}$ is 3109 cm^{-1}, while the splitting of $(15\sigma)^2(16\sigma)^2(8\pi)^4(4\delta)^2(17\sigma)^1$ $a^4\Sigma^-$ is very small, with a term energy 6544 cm^{-1} higher than the ground state. Based on this, the spectroscopic transitions and vibrations for peaks *i*, *l*, and *n* can be identified. Furthermore, we conducted extensive variations in the trapping period and buffer gas density and found that the peaks *j* and *k* in Fig. 3(b) originate from an excited state of the anion. Based on β values and intensities, we assigned peaks *d*, *e*, *j*, *o*, *r*, and *s* to transitions involving a σ orbital photodetachment from the ground state of the anion, leading to X $^3\Sigma_1^-$. Due to limitations in computational hardware and the complexity of anionic states, our MRCI calculations of TaO^- do not align with the experimental data. We tentatively identify peaks *a*–*d* using the states of its isoelectronic TaF as described by Ng *et al.*[62] In addition, benefiting from the ultra-high resolution of the cryo-SEVI method, we re-assigned the peaks in the photoelectron spectra of TaO^- reported by Zheng *et al.*[33] We found that peak M should be assigned to A′ $^2\Pi_{1/2}$, peak O to D $^2\Pi_{1/2}$ rather than B $^2\Phi_{5/2}$, and peak P to C $^2\Delta_{3/2}$ rather than C $^2\Pi_{3/2}$. In addition, we identified previously unassigned peaks A, F, L, N, and Q, following the capital-letter notations used by Zheng *et al.*[33] Detailed results of these assignments are presented in Table III.

Table IV summarizes the experimental and theoretical values for the EAs, vibrational frequencies ω_e, and equilibrium bond lengths r_e for the TaX (X = C, N, O) molecules in comparison with previous studies.

IV. CONCLUSIONS

In conclusion, we investigated the complex states of TaX^- and TaX (X = C, N, O) using the high-resolution cryo-SEVI method jointed with the high-level *ab initio* calculations. We determined EAs of TaC, TaN, and TaO to be 2.098(2), 1.576(2), and 1.069(2) eV, respectively. In addition, the experimental EAs of TaX (X = C, N, O) molecules were compared with values calculated using the CCSD(T)/CBS method. To reliably interpret the experimental spectra, we also conducted MRCI calculations to identify the excited states and determine the vibrational frequencies. We observed several new excited states of these molecules, and some of them cannot be assigned to any known states at the current stage.

Despite the highly accurate CCSD(T)/CBS method, there remains an approximate deviation of 4 kcal/mol between the theoretical calculations and experiments. This discrepancy is attributed to Ta being a 5d metal, requiring the inclusion of spin–orbit coupling and electron correlation effects. Simple scalar relativistic or pseudopotential calculations are not sufficiently accurate. This work can help us understand the 5d transition metal compounds and encourage further experimental and theoretical research into the unique electronic structures of this compound family.

ACKNOWLEDGMENTS

This work was supported by the National Natural Science Foundation of China (NSFC) (Grant Nos. 12374244 and 12341401), the Postdoctoral Fellowship Program of CPSF (Grant No. GZC20231367), and Scientific Research Development Fund Project of the Zhejiang A & F University (Grant No. 2024LFR048).

AUTHOR DECLARATIONS

Conflict of Interest

The authors have no conflicts to disclose.

Author Contributions

Xiaolin Chen: Funding acquisition (equal); Investigation (lead); Writing – original draft (lead); Writing – review & editing (lead). **Shuaiting Yan**: Investigation (supporting). **Rui Zhang**: Investigation (supporting). **Chuangang Ning**: Funding acquisition (equal); Writing – original draft (supporting); Writing – review & editing (lead).

DATA AVAILABILITY

The data that support the findings of this study are available from the corresponding author upon reasonable request.

REFERENCES

[1] A. Fielicke, Chem. Soc. Rev. **52**, 3778 (2023).
[2] J. Shi *et al.*, Nat. Commun. **8**, 958 (2017).
[3] L. S. Xie *et al.*, J. Am. Chem. Soc. **144**, 9525 (2022).
[4] W. Brzezicki, A. M. Oleś, and M. Cuoco, Phys. Rev. X **5**, 011037 (2015).
[5] A. H. J. Cottrell, *Chemical Bonding in Transition Metal Carbides* (CRC Press, London, 1995).
[6] S. J. B. A. Oyama, *The Chemistry of Transition Metal Carbides and Nitrides* (Blackie Academic & Professional, London, 1996).
[7] S. Maekawa *et al.*, *Physics of Transition Metal Oxides* (Springer Science & Business Media, 2013).
[8] V. V. Flambaum, D. DeMille, and M. G. Kozlov, Phys. Rev. Lett. **113**, 103003 (2014).
[9] T. Fleig, M. K. Nayak, and M. G. Kozlov, Phys. Rev. A **93**, 012505 (2016).
[10] O. Krechkivska and M. D. Morse, J. Phys. Chem. A **117**, 13284 (2013).
[11] S. G. Nakhate, S. Mukund, and S. Bhattacharyya, J. Mol. Struct. **1243**, 130888 (2021).
[12] J. Wang, X. Sun, and Z. Wu, J. Cluster Sci. **18**, 333 (2006).
[13] D. Majumdar and K. Balasubramanian, Chem. Phys. Lett. **284**, 273 (1998).
[14] G. Aravind *et al.*, Phys. Rev. A **92**, 042503 (2015).
[15] R. S. Ram, J. Liévin, and P. F. Bernath, J. Mol. Spectrosc. **215**, 275 (2002).
[16] S. Mukund, S. Bhattacharyya, and S. G. Nakhate, Chem. Phys. Lett. **655**, 51 (2016).
[17] J. L. Bouchard, T. Steimle, D. L. Kokkin *et al.*, "Branching ratios, radiative lifetimes, and transition dipole moments for tantalum nitride, TaN," J. Mol. Spectrosc. **325**, 1–6 (2016).
[18] T. Steimle *et al.*, Chem. Phys. Lett. **664**, 138 (2016).
[19] S. G. Nakhate, S. Mukund, and S. Bhattacharyya, Chem. Phys. Lett. **669**, 38 (2017).
[20] T. Steimle *et al.*, J. Chem. Phys. **147**, 154304 (2017).
[21] D. Y. Valdivielso, *Vibrational and Anion Photoelectron Spectroscopy of Transition Metal Clusters* (Technische Universitaet Berlin (Germany), 2022).
[22] C. J. Cheetham and R. F. Barrow, Trans. Faraday Soc. **63**, 1835 (1967).
[23] R. S. Ram and P. F. Bernath, J. Mol. Spectrosc. **191**, 125 (1998).
[24] R. S. Ram and P. F. Bernath, J. Mol. Spectrosc. **221**, 7 (2003).
[25] A. Al-Khalili, U. Hällsten, and O. Launila, J. Mol. Spectrosc. **198**, 230 (1999).
[26] K. J. Manke *et al.*, J. Chem. Phys. **128**, 104302 (2008).
[27] C. R. Christopher, S. Y. Lee, F. B. Gwandu *et al.*, "Rotational and hyperfine analysis of the $E^2\Pi_{1/2}$–$X^2\Delta_{3/2}$ electronic transition of TaO," J. Mol. Spectrosc. **301**, 25–27 (2014).
[28] K. A. Tovar and T. D. Varberg, J. Mol. Spectrosc. **387**, 111666 (2022).
[29] F. Rakowitz *et al.*, J. Chem. Phys. **110**, 3678 (1999).
[30] F. Rakowitz, C. M. Marian, and L. Seijo, J. Chem. Phys. **111**, 10436 (1999).
[31] M. Dolg *et al.*, J. Phys. Chem. **97**, 5852 (1993).
[32] Z. J. Wu, Y. Kawazoe, and J. Meng, J. Mol. Struct.: THEOCHEM **764**, 123 (2006).
[33] W. Zheng, X. Li, S. Eustis, and K. Bowen, "Anion photoelectron spectroscopy of TaO_n^- (n = 1–3)," Chem. Phys. Lett. **460**(1–3), 68–71 (2008).
[34] X. Chen and C. Ning, J. Phys. Chem. Lett. **8**, 2735 (2017).
[35] R. Tang *et al.*, Phys. Rev. Lett. **123**, 203002 (2019).
[36] J. Czekner and L. S. Wang, J. Phys. Chem. A **124**, 10001 (2020).
[37] M. C. Babin *et al.*, J. Chem. Phys. **155**, 114305 (2021).
[38] C. Ning and Y. Lu, J. Phys. Chem. Ref. Data **51**, 021502 (2022).
[39] D. M. Neumark, J. Phys. Chem. A **127**, 4207 (2023).
[40] G. S. Kocheril, H. W. Gao, and L. S. Wang, J. Chem. Phys. **158**, 236101 (2023).
[41] Z. Luo *et al.*, Phys. Rev. A **93**, 020501 (2016).
[42] R. Tang, X. Fu, and C. Ning, J. Chem. Phys. **149**, 134304 (2018).
[43] Y. Lu *et al.*, Chin. Phys. Lett. **40**, 093101 (2023).
[44] W. C. Wiley and I. H. McLaren, Rev. Sci. Instrum. **26**, 1150 (1955).
[45] B. Dick, Phys. Chem. Chem. Phys. **16**, 570 (2014).
[46] J. Cooper and R. N. Zare, J. Chem. Phys. **48**, 942 (1968).
[47] J. Cooper and R. N. Zare, J. Chem. Phys. **49**, 4252 (1968).
[48] Y. Liu and C. Ning, J. Chem. Phys. **143**, 144310 (2015).
[49] R. A. Kendall, T. H. Dunning, and R. J. Harrison, J. Chem. Phys. **96**, 6796 (1992).
[50] D. Figgen and P. Schwerdtfeger, J. Chem. Phys. **130**, 164108 (2009).
[51] R. J. Bartlett *et al.*, Chem. Phys. Lett. **165**, 513 (1990).
[52] M. Frisch *et al.*, GAUSSIAN 09, revision B.01 (Gaussian, Inc., Wallingford, CT, 2009).
[53] K. A. Peterson, D. E. Woon, and T. H. Dunning, J. Chem. Phys. **100**, 7410 (1994).
[54] T. Helgaker *et al.*, J. Chem. Phys. **106**, 9639 (1997).
[55] D. Feller, K. A. Peterson, and T. D. Crawford, J. Chem. Phys. **124**, 054107 (2006).
[56] D. Feller and K. A. Peterson, J. Chem. Phys. **126**, 114105 (2007).
[57] H. J. Werner *et al.*, Wiley Interdiscip. Rev.: Comput. Mol. Sci. **2**, 242 (2012).
[58] S. R. Langhoff and E. R. Davidson, Int. J. Quantum Chem. **8**, 61 (1974).
[59] A. Berning *et al.*, Mol. Phys. **98**, 1823 (2000).
[60] J. P. Araújo and M. Y. Ballester, Int. J. Quantum Chem. **121**, e26808 (2021).
[61] M. Zhou and L. Andrews, J. Phys. Chem. A **102**, 8251 (1998).
[62] K. F. Ng *et al.*, J. Chem. Phys. **146**, 094308 (2017).
[63] B. Hong, L. Cheng, M. Y. Wang, and Z. J. Wu, "Electronic structures and chemical bonding in 4d- and 5d-transition metal mononitrides," Mol. Phys. **108**(1), 25–33 (2010).
[64] M. Zhou and L. Andrews, J. Phys. Chem. A **102**, 9061 (1998).